International Journal of Current Advanced Research
ISSN: O: 2319-6475, ISSN: P: 2319-6505, Impact Factor: 6.614
Available Online at www.journalijcar.org
Volume 7; Issue 10(E); October 2018; Page No. 16051-16057
DOI: http://dx.doi.org/10.24327/ijcar.2018.16057.2947

Research Article

AN ATOMISTIC STUDY ON THE ROLE OF GRAIN BOUNDARY SEGREGATED CARBON AND NITROGEN ON THE TENSILE PROPERTIES OF NANOCRYSTALLINE FERRITE

Ahmed Tamer AlMotasem

Department of Physics, Faculty of Science, Assiut University, 71516 Assiut, Egypt

A R T I C L E I N F O

Article History:

Received 12th July, 2018
Received in revised form 23rd August, 2018
Accepted 7th September, 2018
Published online 28th October, 2018

Key words:

ferrite, molecular dynamics, segregation, stacking fault, dislocation, twinning

A B S T R A C T

Several experimental reports have shown that segregated carbon and nitrogen have slightly different roles on the strength of ferriticsteels; however, the mechanistic origin of this behavior is not yet clearly understood. In the present work, large scale molecular dynamics (MD) simulations were used to explore the effect of segregated carbon and nitrogen on the deformation behavior of nanocrystalline (nc) ferrite. The deformation mechanisms associated with plasticity during tensile test were analyzed. It is found that, at low strain, grain boundary (GB) sliding mediated plasticity is dominated, whereas dislocation activity and deformation twinning are the primary deformation mechanisms at high strain. The results reveal that the segregation of carbon or nitrogen leads to a significant reduction of GBs dislocations. Besides, the stress required for twinning nucleation was found to strongly depend on the segregated solute type. The flow stress increases for both cases; however, nitrogen has a relatively small impact compared to carbon. The competition between different deformation mechanisms was interpreted by stable stacking fault, unstable stacking fault as well as unstable twinning fault energies. The simulation results were compared to the available experimental data and models and a fair agreement was found.

INTRODUCTION

Nanocrystalline (nc) metals have attracted increasingly great attention due to their superior mechanical properties and their potential for high strength applications materials. The de for mation behavior and fracture of nanocrystal line materials are significantly driven by grain boundaries (GBs) and their underlying structure (Gleiter, 1982; Wolf, 1989).Thus, achieving a high level of (nc) metals strengthen could be accomplished by either alloying or enriching grain boundary using suitable dopants. In literature several previous studies have shown that alloying and GB segregation can improve the strength of (nc) metals by preventing grain growth, as evidenced by the enhanced thermal stability of a number of binary nanocrystalline alloys relative to their single-component counterparts (Detor and Schuh, 2007; Ebrahimi and Li, 2006; Günther *et al*., 1992; Hibbard *et al*., 2006; Li and Ebrahimi, 2003; Weissmüller *et al*., 1995).For example, in ferritic steels(Takaki, 2010; Takaki *et al*., 2014; Takeda *et al*., 2008), experimental observations have revealed that adding carbon and nitrogen leads to an increase of their yield strength and the Hall-Petch (HP)coefficient increased greatly from 100 to 600 MPa. $\mu m^{-1/2}$, depending on the solute carbon content, while the (HP) coefficient was barely influenced by adding nitrogen.

Corresponding author:* **Ahmed Tamer AlMotasem
Department of Physics, Faculty of Science, Assiut University, 71516 Assiut, Egypt

In an attempt to explain the differences between the role of carbon and nitrogen on the (HP) coefficient, Takahashi *et al*. (Takahashi *et al*., 2012) have demonstrated that, using atom probe tomography (APT), although both nitrogen and carbon have a similar tendency to segregate at the boundary of ferritic steel, the coefficient increment per unit interfacial excess for nitrogen is lower compared to that of carbon which may explain that why nitrogen has a little influence on the ferrite strength. On the other hand, theoretical first-principles results by Wu *et al*. (Wu *et al*., 1996) reveal that carbon acts as cohesion enhancer in bcc-Fe grain boundary while nitrogen weakens GBs(Matsumoto *et al*., 2011).

Similarly, in austenite steels, the electron backscatter diffraction (EBSD)observations, by Takuro *et al*.(Masumura *et al*., 2015), reveal the differences in deformation microstructure between carbon/nitrogen-addedaustenitic steels. For example, it was reported that adding carbon promotes deformation twins and ε-martensite transformation while the dislocation activities are more favorable in the case of nitrogen-added austenitic steels. They attributed such behavior to the differences in stacking fault energy (SFE) between carbon/nitrogen added-steels.

In spite of the abundant experimental studies which provide strong indication that carbon and nitrogen segregation to GBs can improve strength of (nc) ferrite. However, the role of carbon and nitrogen on the onset plasticity of ferrite is not yet completely understood. In the present work, with the development of classical interatomic potentials for both Fe-C

and Fe-N, we utilize the large-scale atomistic simulations to investigate the effect of adding carbon and nitrogen into ferritic steel on the deformation behavior of ferrite. Such investigations are crucial to practically realize their potential properties for mechanical applications.

Simulation Details

Nanocrystalline iron sample, depicted in Fig.1,was constructed following the Voronoi tessellation method(Voronoi, 2009), implemented within Atomsk tool (Hirel, 2015).In this method, a sample with average grain size, D =14.12 nm, was built by filling in a cubic box with randomly distributing seeds then a bcc lattice grains with random misorientations generated from the seeds. The simulation box has size of 350×210×170 $Å^{3,}$ aligned with –x, -y and –z directions, respectively, containing about 1,100,000 atoms. In order to eliminate free surface effects, the simulation cell is periodic in all directions. Also, the overlapped atoms within 0.7 distances have been deleted to eliminate the initial undesirable artificial defects which may arise from constructing the model. The identification of lattice and non–lattice atoms, including grain boundary atoms, was made via common neighbor analysis (Honeycutt and Andersen, 1987). Thus, it allows for inserting alloying elements into grain boundary. In the previous MD studies, the distribution of foreign atoms within the grain boundary was either randomly or by hybrid MC/MD approach(Caro *et al*., 2010; Schäfer *et al*., 2011). In this work, carbon or nitrogen solute atoms, with an average composition 2.5 %, were randomly placed in the GBs and only the solute type was changed whereas the position and the concentration of alloying elements were kept. In the recent atom probe tomography (APT) study (Takahashi *et al*., 2012), it has been shown both nitrogen and carbon tends to segregate with a similar amount at GBs of ferritic steel. Thus, the insertion of carbon or nitrogen atoms in GB in equal amount is justified.

The system was initially equilibrated at 0K using the conjugate gradient method. Then, the system is thermally equilibrated to 300 K and 0 GPa pressure for 100ps using isobaric/isothermal NPT ensemble to ensure stress-free state. The time step of 1 fs was chosen for our simulations. During dynamic loading, the sample is subjected to uniaxial tensile with constant strain rate, 5×10^{8} s^{-1},along x direction whereas the pressure in both –y and –zdirections is kept zero. The MD strain rate is considerably high compared to the lab experiments, however, it is sufficient to capture grain boundary mediated as well as dislocations plastic deformation.

The interaction between Fe-C(Lee, 2006) and Fe-N(Lee *et al*., 2006) atoms is described by the second nearest neighbor modified embedded atom method (2NN-MEAM)potentials. The potentials parameters were developed by fitting to the experimental data of Fe-C and Fe-N dilute systems. The potentials can be used reliably to simulate the interactions between carbon and nitrogen interstitials with dislocations and grain boundaries and to investigate the effects of carbon and nitrogen on various deformation and mechanical behaviors of bcc/fcciron.

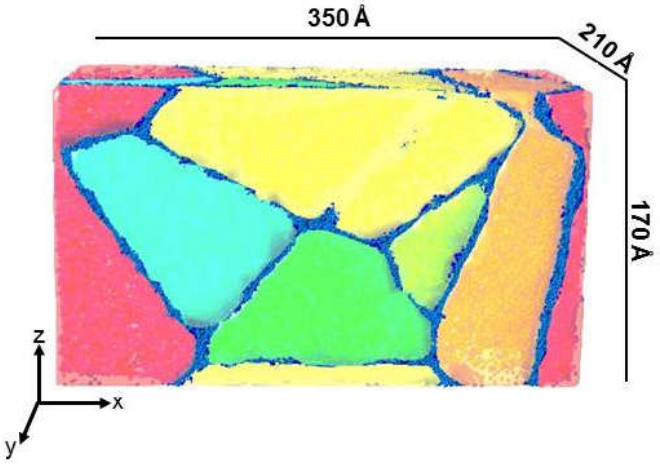

Fig 1 Snapshot of MD simulation model of (nc) ferrite, grain boundaries are colored in dark blue.

During tensile simulation, the identification of dislocations was made via dislocation extraction algorithm (DXA) (Stukowski and Albe, 2010),while the structural defects was analyzed by Crystal Analysis Tool (CAT), based on adaptive common-neighbor analysis, developed by Stukowski *et al*. (Stukowski, 2012; Stukowski and Arsenlis, 2012). Visualization of all MD simulation snapshots were made via the open source software Ovito(Stukowski, 2010) and Atom Viewer (Begau *et al*., 2012, 2011).

In order to simulate the generalized planer fault energy (GPFE) and determine the value of the stable fault energy (γ_{sf}), the unstable fault (γ_{usf}), the unstable twinning fault (γ_{utf}), a bcc-Fe lattice was created and oriented along the [1 1 1], [1 12] and [1 1 0] directions. The solute atoms were randomly placed in the octahedral site of bcc lattice, as it has been shown this octahedral site is energetically more favorable for carbon and nitrogen interstitial site(Kaufman and Bernstein, 1970; Porter and Easterling, 1992; Saunders and Miodownik, 1998). Then the simulation box was minimized using conjugate gradient (CG) method to ensure the stress-free state of initial configuration before shearing. The periodic boundary condition was invoked in the lateral direction, i.e in the [111] and [$\bar{1}$10]directions. The simulation box was initially divided into upper and lower regions in the [112] direction. Then, the atoms in the upper region were rigidly displaced by a displacement of $b_p = 1/6\langle 111\rangle$. Then, a new upper region including the next layer to the previously sheared layers, again is displaced by $2b_p$.

RESULTS AND DISCUSSION

Here, before applying the tensile deformation, the as-prepared samples were undergone thermal annealing at 300 K for 200 ps. This procedure is important to allow the system to relax and remove undesired high energy configurations. Thus, we focus only on the role of the grain boundary segregation to the strength of nanocrystalline samples. Fig. 2 illustrates the influence of segregated atoms on the potential energy per atom for different (nc) samples.

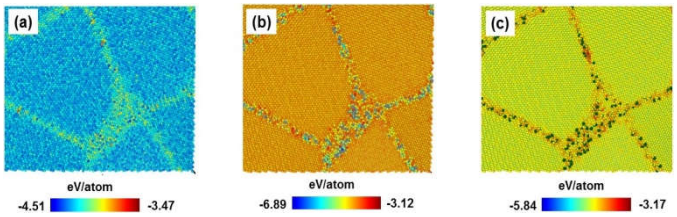

Fig 2 Sliced snapshots showing the variation of potential energy per atom for different segregated solute types, a) pure iron, b) Fe-C and c) Fe-N, obtained by the end of annealing stage. (For interpretation of the references to color in this figure, the reader is referred to the web version of this article).

In order to quantitatively assess the effect of the segregated atoms on the material strength, we have estimated the specific GB energy (E_{GB}) (Millett *et al*., 2006; Vo *et al*., 2011), defined as the excess GB energy per GB atoms, see Table 1.

Table 1 Specific GB energies (E_{GB}) for (nc) Fe samples with N or C solute atoms.

(nc) Sample	E_{GB} (eV/atom)
Fe	0.17
Fe-C	0.02
Fe-N	0.15

It can be seen that, while the value of (E_{GB}) for Fe-N sample slightly reduced from that of pure (nc) ferrite sample, a tremendous decrease of the (E_{GB}) was obtained for (nc) Fe-Cby factor of about 9 compared to that of (nc) ferrite sample. Our findings are in line with the results of Density Function theory (DFT) where it is reported that carbon and nitrogen improve the cohesion of GB in bcc-Fe(Fen and Wang, 2001; Matsumoto *et al*., 2011).

On the other hand, the results of (DXA) analysis, as illustrated in Fig. 3, reveal the absence of intragranular dislocations in all samples, while the grain boundaries (GBs) dislocations are observed only in the case of (nc) Fe. Besides, we also noticed that further annealing for longer time does not change the GBs dislocation densities for (nc) Fe. Unlike the case of pure (nc) Fe, no GBs dislocations were observed for the nc sample with segregated solute atoms.

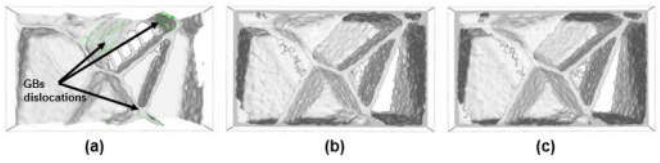

Fig 3 Nanocrystalline samples obtained after annealing at 300 K for 100 ps. (a) Fe, (b) Fe-C and (c) Fe-N. Atoms are omitted for better visualization.

This result suggests that the segregated carbon and nitrogen suppress the formation of dislocation at GBs and therefore may enhance the strength of the GBs. Indeed, the present results support the explanation given by Takaki (Takaki, 2010), following Cottrell's model(Cottrell, 1964), in whichit is assumed that segregated carbon and nitrogen stabilized the dislocation emission site at grain boundary and leads to high stress concentration at GBs.

Stress-Strain curves of (nc) samples

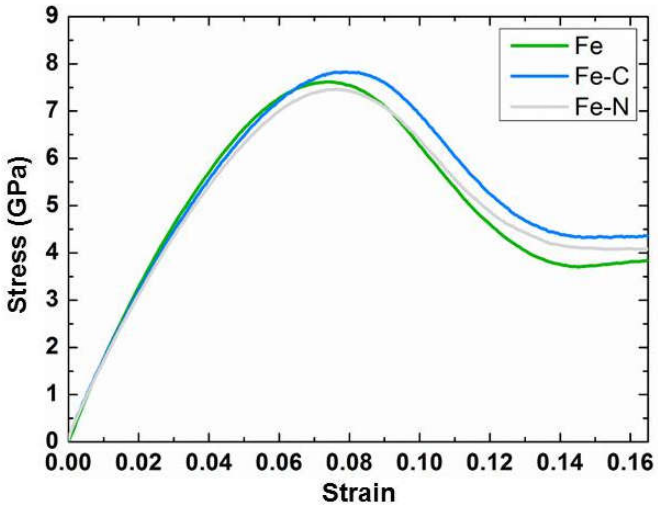

Fig 4 Typical stress-strain curves during tensile deformation of (nc) samplesat strain rate 5×10^{8} s^{-1}.

Fig 4. shows the results of tensile test up to strain about 16 % for all samples considered in this work. Initially, the stress increases with strain up to peak stress about 7.61, 7.82 and 7.46 GPa corresponding to Fe, Fe-C and Fe-N nanocrystalline samples, respectively. It is worth mentioned here, the value of the peak stress is greatly amplified compared to corresponding experimental values (Takaki, 2010; Takeda *et al*., 2008)due to high strain rate inherent in MD simulation. In order to investigate the effect of segregated solute type on the material strength, the average flow stress is rather used, where the stress is insensitive to the strain rate. The value of the flow stress was obtained by averaging the total stress over strain interval14-16%. The values of average flow stress are 3.77, 4.34 and 4.08 GPa for Fe, Fe-C and Fe-N nanocrystalline samples, respectively. In general, we found that both elements carbon and nitrogen lead to increase of the material strength. However, while carbon increases of the value of the σ_{flow} by about 15% whereas nitrogen has relatively small effect as it increases the σ_{flow} by about 8%.These findings are in a fair agreement with the experimental studies carried out by (Takaki *et al*., 2014; Takeda *et al*., 2008).

Effect of carbon/nitrogen segregation on the plastic deformation processes

In the following we shall characterize the deformation mechanisms associated with the plasticity of (nc) samples using (CAT).As shown in Fig. 4, the stress-strain curves exhibit linearity up to 2 % strain above this strain value a deviation from linearity to non-linearity is observed. The results from (CAT) analysis reveal no dislocations or twins activities at this low strain. Thus, it is assumed the deformation mechanism in this stage is rather due to GB activities. We examine this assumption by calculating the local atomic strain distribution for both lattice and non-lattice atoms, as illustrated in Fig. 5(c). Obviously, the atomic strain is largely localized at GBs, in comparison to grain interior atoms. Additionally, it can be seen that the samples with GB segregated carbon or nitrogen exhibit high localized atomic strain compared to that (nc) ferrite. In order to further elucidate the effect segregated solute type on the amount of atomic strain, we have plotted the probability density of ε_{xx}, for the lattice and none-lattice

atoms as shown in Fig. 5 (a-b). Clearly, the highest atomic strain for the lattice atoms is obtained for pure(nc) ferrite, whereas the highest strain for non-lattice atoms is observed for (nc) sample with segregated solute atoms. Note the difference of ε_{xx} scale between the lattice atoms and the non-lattice atoms is about an order of magnitude. This result confirms that GB sliding is dominated at this early stage of deformation.

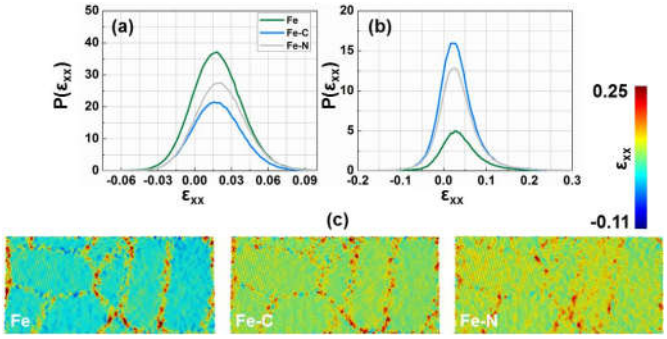

Fig. 5. The probability distribution of strain P(ε_{xx}) for , a) grain interior atoms and b) grain boundary atoms obtained via common neighbor analysis (CNA), c) sliced snapshot displays the atomic level distribution (ε_{xx}) corresponding to each sample.(Forinterpretationofthereferencestocolorinthis figure,thereaderisreferredtothewebversionofthisarticle.).

At large total strains, see Figs.6-8,various deformation mechanisms including, GB dislocation emission, twins nucleation at grain boundary, phase transformation and formation of vacancies and interstitial clusters were observed.In the following we have investigated the effect of segregated alloying elements on the different deformation mechanisms observed during tensile simulation. For instance, the effect of carbon/nitrogen addition on the dislocation density is illustrated in Fig. 9(a). In General, two kinds of dislocations which are commonly observed in bcc-Fe were found, namely dislocations with Burgers vectors $\frac{1}{2}\langle 111\rangle$ and $\langle 100\rangle$ (Kelly and Knowles, 2012).

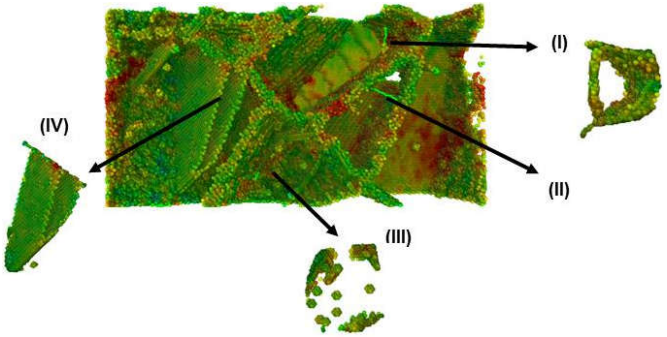

Fig 6 Concurrent various deformation mechanisms observed during tensile load of (nc) Fe sample. I) nucleation of GB dislocation, II) nucleation of twins at GB. III) Twinning growth within grain interior and IV) formation of vacancies and interstitial clusters. Coloring of atoms due to their von mises stress. (For interpretation of the references to color in this figure, the reader is referred to the web version of this article).

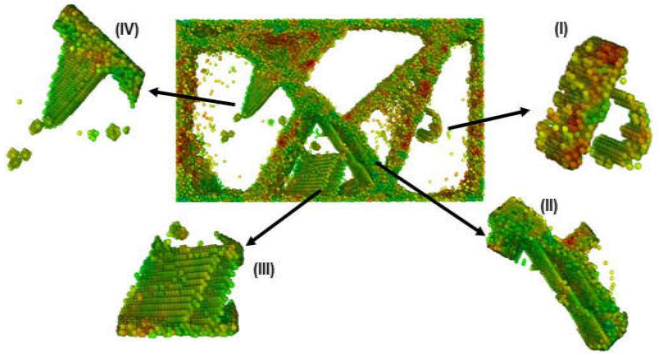

Fig 7 Concurrent various deformation mechanisms observed during tensile load of Fe-C sample. I) nucleation of GB dislocation, II) nucleation of twins at GB. III) twinning growth within grain interior and IV) formation of vacancies and interstitial clusters. (For interpretation of the references to color in this figure, the reader is referred to the web version of this article).

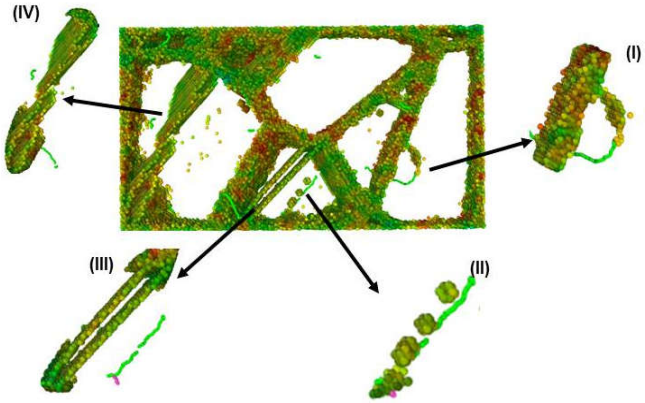

Fig 8 Concurrent various deformation mechanisms observed during tensile load of (nc) Fe-N sample. I) nucleation of GB dislocation, II) dislocation expansion within grain interior. III) extension of twinning region inside grain, IV) formation of vacancies and interstitial clusters. (For interpretation of the references to color in this figure, the reader is referred to the web version of this article.).

From Figs. (6-8), two important aspects can be highlighted, i) the pre-existing dislocations are only observed in the case of (nc) iron and ii) the dislocation nucleation of (nc) Fe-C and (nc) Fe-N occurs at higher strain compared to that of (nc) Fe. It is found that the nucleation of dislocation in(nc)samples containing nitrogen or carbon occurs at strain ε =0.068 and ε =0.075, respectively. However, with further strain the differences in dislocation densities among three samples become indistinguishable. Thus, we can assume that both carbon and nitrogen play a key role on the nucleation of dislocations. Similarly, for all (nc) samples, the twinning initiates at the grain boundaries (GBs) then propagates inside the grain interior. Note that, depending on the orientation and the size of grain, the twinning initiation and growth is preferentially observed in certain grains, see Figs. (6-8). Fig. 9(b) presents the variation of twining fraction with strain. It can be noticed that, in the case of (nc) Fe-C and (nc)Fe-N the twins nucleate at higher strains compared to (nc) Fe.

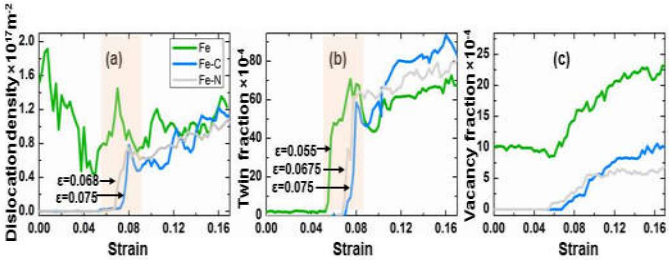

Fig 9 Evolution of a) dislocation density, b) twin fraction and c) vacancy fractions with applied strain for different (nc)samples.

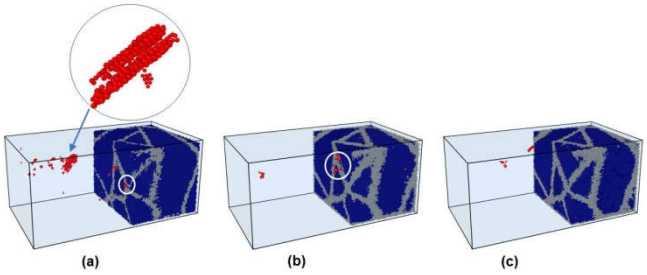

Fig 10 Atomistic snapshot showing the spatial distribution of twins corresponding to different samples, a) Fe, b) Fe-C and c) Fe-N nanocrystalline samples. Blue and grey atoms denote lattice and non-lattice atoms, respectively. White circles mark the nucleation of twin at GBs. (For interpretation of the references to color in this figure, the reader is referred to the web version of this article).

In order to further elucidate the role of segregated carbon or nitrogen on deformation mechanisms associated with plasticity of ferritic steels, we investigated the influence of carbon and nitrogen on the generalized planer fault energy (GPFE) of bcc-Fe single crystal. The GPFE curve can accurately provide the value of the stable fault energy (γ_{sf}), the unstable fault (γ_{usf}), the unstable twinning fault (γ_{utf}). These values, listed in Table. 2, are important to determine the competition among deformation mechanisms.

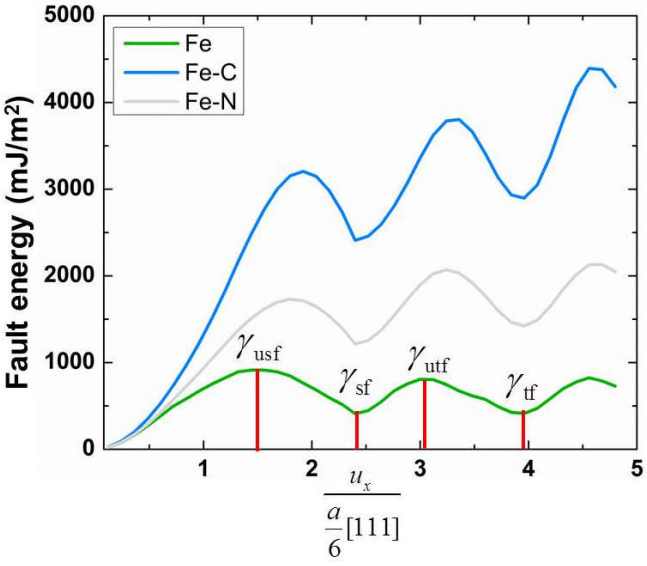

Fig 11 Influence of carbon/ and nitrogen on the generalized planner fault energy curve (GPFE) of bcc-Fe single crystal.

From Table 2, adding carbon or nitrogen to bcc-Fe leads to a significant increase of γ_{sf}, γ_{usf} and γ_{utf} values. Moreover, the ratios (γ_{usf}/γ_{sf}) and ($\gamma_{utf}/\gamma_{usf}$), which are related to the energy barrier for dislocation nucleation and twinning nucleation, respectively, were calculated. Obviously, the lowest value of (γ_{usf}/γ_{sf}) and ($\gamma_{utf}/\gamma_{usf}$) are obtained for bcc-Fe. On the other hand, the ratio of (γ_{usf}/γ_{sf}) of (nc) Fe-N is relatively smaller than that of (nc) Fe-C suggesting that dislocation generation is energetically more favorable whereas the ratio ($\gamma_{utf}/\gamma_{usf}$) is lower in the case of Fe-C promoting deformation via twinning. Indeed, the results presented in Figs. (7) and (8) clearly show that dislocation activity is more pronounced in (nc) Fe-N while twins frequently form in the case of (nc) Fe-C. Our simulation results on the role of carbon and nitrogen in ferritic steels coincide with those obtained for austenitic steels. For instance, the results of Electron Back Scatter Diffraction (EBSD) on the impact of adding carbon or nitrogen to austenitic steels reveal that dislocation accumulation was more significant in the nitrogen-added steel, whereas deformation twins were more frequently formed in the carbon-added steel (Yoshitake *et al*., 2012). On the other hand, according to the pole mechanism proposed by Cottrell and Bilby (Cottrell and Bilby, 1951), the critical nucleation twinning stress is given by $\tau_o = \frac{\gamma_{usf}}{b}$, where b is the dislocation Burgers vector. The calculated values of τ_o are 0.37, 1.31, 0.71 GPa for Fe, Fe-C and Fe-N nanocrystalline samples, respectively. Interestingly, the calculated values of τ_o for (nc)Fe is close to the typical experimental value of body-centered cubic iron (< 0.5 GPa, (de Rességuier and Hallouin, 1998; Meyers *et al*., 2001)).

The above results suggest that carbon and nitrogen play a significant role during the nucleation stage of twins; however, with further increase of strain the twins growth becomes insensitive to segregated atoms. Thus, the twin growth can be considered as strain-induced rather than solute atoms GBs segregation. Such a behavior is plausible since the values of γ_{sf}, γ_{usf} and γ_{utf} are strongly stress-dependent as has been illustrated by Liang *et al*. (Liang *et al*., 2015).

Table 2 Values of γ_{sf}, γ_{usf} and γ_{utf} corresponding to (nc) Fe, Fe-C and Fe-N samples.

	γ_{usf} mJ/m²	γ_{sf} mJ/m²	γ_{utf} mJ/m²	γ_{usf}/γ_{sf}	$\gamma_{utf}/\gamma_{usf}$
Fe	912	410	805	0.44956	0.88268
Fe-C	3205	2408	3660	0.75133	1.14197
Fe-N	1730	1213	2070	0.70116	1.19653

Finally, as illustrated in Fig.12, during tensile test the formation of vacancy nanoclusters was observed. Obviously, the fraction of vacancies is more pronounced in the absence of segregated solutes. The detailed analysis of vacancies fraction with strain, cf. Fig.9(c) indicates that the onset of vacancies formation occurs at higher strain compared to pure ferrite. Thus, the presence of carbon and nitrogen suppresses the formation of vacancies. It is noticed also that the strains at which the vacancy formation starts are comparably equal to the strains at which twins or dislocations nucleate. In fact the formation of vacancies during deformation, shown in Figs.6-8, is not surprising as they may be result either from a rough motion of a dislocation under high stress, Fig. 8(II), which eventually leads to the formation of lattice defects as reported in Ref. (Marian *et al*., 2004), or from the deformation twins, Fig. 7(IV), as experimentally observed by electron microscopy of high-speed deformation of metals and later explained by Segeer (Seeger, 2007).

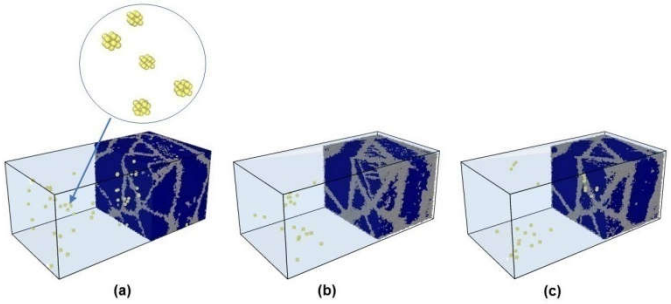

Fig 12 Atomistic snapshot showing the spatial distribution of vacancies corresponding to different samples, a)Fe, b)Fe-C and c)Fe-N nanocrystalline samples. Blue, grey and yellow colors mark lattice, non-lattice atoms and vacancies, respectively. (For interpretation of the references to color in this figure, the reader is referred to the web version of this article).

CONCLUSION

In the present study we performed MD simulations to explore the role of grain boundary segregated carbon and nitrogenon the plasticity ofnanocrystalline ferrite. We found that the value of E_{GB} was affected by the segregated solute type. For instance, a tremendous decrease of E_{GB} value is obtained by adding carbon whereas nitrogen slightly reduces E_{GB}. In contrast to pure (nc) ferrite, a fully GBs dislocations suppression is observed for samples with segregated solute atom at GB. We found that, at early stage of plasticity, GB sliding is dominant while at large strain both dislocation activity and deformation twinning are the primary deformation mechanisms. In general, both of dislocation nucleation or deformation twinnings originate from the grain boundary. However, the nucleation of either dislocations or twins is significantly affected by segregated atoms. The competition between dislocation and twins was explained in terms of stacking and twinning fault energies. The simulation results of GPFE curves clearly show that the values of stacking and twinning fault energies vary considerably with carbon and nitrogen.

Acknowledgement

We are grateful to the High Availability Super Computing Center at Assiut University (HASCC)for providing computational resources.

References

Begau, C., Hartmaier, A., George, E.P., Pharr, G.M., 2011. Atomistic processes of dislocation generation and plastic deformation during nanoindentation. Acta Mater. 59,934–942. https://doi.org/10.1016/j.actamat.2010.10.016

Begau, C., Hua, J., Hartmaier, A., 2012. A novel approach to study dislocation density tensors and lattice rotation patterns in atomistic simulations. *J. Mech. Phys. Solids* 60, 711–722. https://doi.org/10.1016/j.jmps.2011.12.005

Caro, A., Farkas, D., Bringa, E.M., Gilmer, G.H., Zepeda-Ruiz, L.A., 2010. Effects of Microalloying on the Mobility and Mechanical Response of Interfaces in Nanocrystalline Cu. Mater. Sci. Forum 633–634, 21–30. https://doi.org/10.4028/www.scientific.net/MSF.633-634.21

Cottrell, A.H., 1964. The mechanical properties of matter. Wiley, New York, pp. 272–283.

Cottrell, A.H., Bilby, B.A., 1951. LX. A mechanism for the growth of deformation twins in crystals. Lond. Edinb. Dublin Philos. Mag. *J. Sci.* 42, 573–581. https://doi.org/10.1080/14786445108561272

de Rességuier, T., Hallouin, M., 1998. Stress relaxation and precursor decay in laser shock-loaded iron. *J. Appl. Phys.* 84, 1932–1938. https://doi.org/10.1063/1.368322

Detor, A.J., Schuh, C.A., 2007. Tailoring and patterning the grain size of nanocrystalline alloys. Acta Mater. 55, 371–379. https://doi.org/10.1016/j.actamat.2006.08.032

Ebrahimi, F., Li, H., 2006. Grain growth in electrodeposited nanocrystalline fcc Ni–Fe alloys. Scr. Mater. 55, 263–266. https://doi.org/10.1016/j.scriptamat.2006.03.053

Fen, Y.-Q., Wang, C.-Y., 2001. Electronic effects of nitrogen and phosphorus on iron grain boundary cohesion. Comput. Mater. Sci. 20, 48–56. https://doi.org/10.1016/S0927-0256(00)00124-5

Gleiter, H., 1982. On the structure of grain boundaries in metals. Mater. Sci. Eng. 52, 91–131. https://doi.org/10.1016/0025-5416(82)90040-4

Günther, B., Kumpmann, A., Kunze, H.-D., 1992. Secondary recrystallization effects in nanostructured elemental metals. Scr. Metall. Mater. 27, 833–838. https://doi.org/10.1016/0956-716X(92)90401-Y

Hibbard, G.D., Aust, K.T., Erb, U., 2006. Thermal stability of electrodeposited nanocrystalline Ni–Co alloys. Mater. Sci. Eng. A 433, 195–202. https://doi.org/10.1016/j.msea.2006.06.096

Hirel, P., 2015. Atomsk: A tool for manipulating and converting atomic data files. Comput. Phys. Commun. 197, 212–219. https://doi.org/10.1016/j.cpc.2015.07.012

Honeycutt, J.D., Andersen, H.C., 1987. Molecular dynamics study of melting and freezing of small Lennard-Jones clusters. *J. Phys. Chem.* 91, 4950–4963. https://doi.org/10.1021/j100303a014

Kaufman, L., Bernstein, H., 1970. Computer Calculation of Phase Diagrams with Special Reference to Refractory Metals. Academic Press.

Kelly, A., Knowles, K.M., 2012. Crystallography and Crystal Defect, second. ed. John Wiley & Sons, Ltd.

Lee, B.-J., 2006. A modified embedded-atom method interatomic potential for the Fe–C system. Acta Mater. 54, 701–711. https://doi.org/10.1016/j.actamat.2005.09.034

Lee, B.-J., Lee, T.-H., Kim, S.-J., 2006. A modified embedded-atom method interatomic potential for the Fe–N system: A comparative study with the Fe–C system. Acta Mater. 54, 4597–4607. https://doi.org/10.1016/j.actamat.2006.06.003

Li, H.Q., Ebrahimi, F., 2003. An investigation of thermal stability and microhardness of electrodeposited nanocrystalline nickel-21% iron alloys. Acta Mater. 51, 3905–3913. https://doi.org/10.1016/S1359-6454(03)00215-5

Liang, Z., Lü, C., Tieu, K., Xing, Z., Lin-Qing, P., Michal, G., 2015. Molecular dynamics simulation on generalized stacking fault energies of FCC metals under preloading stress. Chin. Phys. B 24, 088106.

Marian, J., Cai, W., Bulatov, V.V., 2004. Dynamic transitions from smooth to rough to twinning in

dislocation motion. Nat. Mater. 3, 158–163. https://doi.org/10.1038/nmat1072

Masumura, T., Nakada, N., Tsuchiyama, T., Takaki, S., Koyano, T., Adachi, K., 2015. The difference in thermal and mechanical stabilities of austenite between carbon- and nitrogen-added metastable austenitic stainless steels. Acta Mater. 84, 330–338. https://doi.org/10.1016/j.actamat.2014.10.041

Matsumoto, R., Riku, M., Taketomi, S., Miyazaki, N., 2011. Hydrogen–Grain Boundary Interaction in Fe, Fe–C, and Fe–N Systems. Prog. Nucl. Sci. Technol. 2, 9–15. https://doi.org/10.15669/pnst.2.9

Meyers, M.A., Vöhringer, O., Lubarda, V.A., 2001. The onset of twinning in metals: a constitutive description. Acta Mater. 49, 4025–4039.

Millett, P.C., Selvam, R.P., Saxena, A., 2006. Molecular dynamics simulations of grain size stabilization in nanocrystalline materials by addition of dopants. Acta Mater. 54, 297–303. https://doi.org/10.1016/j.actamat.2005.07.024

Porter, D.A., Easterling, K.E., 1992. Phase Transformations in Metals and Alloys, Third Edition (Revised Reprint). CRC Press.

Saunders, N., Miodownik, A.P., 1998. CALPHAD (Calculation of Phase Diagrams): A Comprehensive Guide. Elsevier.

Schäfer, J., Stukowski, A., Albe, K., 2011. Plastic deformation of nanocrystalline Pd–Au alloys: On the interplay of grain boundary solute segregation, fault energies and grain size. Acta Mater. 59, 2957–2968. https://doi.org/10.1016/j.actamat.2011.01.036

Seeger, A., 2007. Production of lattice vacancies in metals by deformation twinning. Philos. Mag. Lett. 87, 95–102. https://doi.org/10.1080/09500830601123801

Stukowski, A., 2012. Structure identification methods for atomistic simulations of crystalline materials. Model. Simul. Mater. Sci. Eng. 20, 045021. https://doi.org/10.1088/0965-0393/20/4/045021

Stukowski, A., 2010. Visualization and analysis of atomistic simulation data with OVITO–the Open Visualization Tool. Model. Simul. Mater. Sci. Eng. 18, 015012. https://doi.org/10.1088/0965-0393/18/1/015012

Stukowski, A., Albe, K., 2010. Extracting dislocations and non-dislocation crystal defects from atomistic simulation data. Model. Simul. Mater. Sci. Eng. 18, 085001. https://doi.org/10.1088/0965-0393/18/8/085001

Stukowski, A., Arsenlis, A., 2012. On the elastic–plastic decomposition of crystal deformation at the atomic scale. Model. Simul. Mater. Sci. Eng. 20, 035012. https://doi.org/10.1088/0965-0393/20/3/035012

Takahashi, J., Kawakami, K., Ushioda, K., Takaki, S., Nakata, N., Tsuchiyama, T., 2012. Quantitative analysis of grain boundaries in carbon- and nitrogen-added ferritic steels by atom probe tomography. Scr. Mater. 66, 207–210. https://doi.org/10.1016/j.scriptamat.2011.10.026

Takaki, S., 2010. Effect of Carbon and Nitrogen on the Hall-Petch Coefficient of Ferritic Iron (Review on the Hall-Petch Relation in Ferritic Iron). Mater. Sci. Forum 638–642, 168–173. https://doi.org/10.4028/www.scientific.net/MSF.638-642.168

Takaki, S., Akama, D., Nakada, N., Tsuchiyama, T., 2014. Effect of Grain Boundary Segregation of Interstitial Elements on Hall–Petch Coefficient in Steels. Mater. Trans. 55, 28–34.

Takeda, K., Nakada, N., Tsuchiyama, T., Takaki, S., 2008. Effect of interstitial elements on Hall-Petch coefficient of ferritic iron. ISIJ Int. 48, 1122–1125.

Vo, N.Q., Schäfer, J., Averback, R.S., Albe, K., Ashkenazy, Y., Bellon, P., 2011. Reaching theoretical strengths in nanocrystalline Cu by grain boundary doping. Scr. Mater. 65, 660–663. https://doi.org/10.1016/j.scriptamat.2011.06.048

Voronoi, G., 2009. Nouvelles applications des paramètres continus à la théorie des formes quadratiques. Deuxième mémoire. Recherches sur les parallélloèdres primitifs. J. Für Reine Angew. Math. Crelles J. 1908, 198–287. https://doi.org/10.1515/crll.1908.134.198

Weissmüller, J., Löffler, J., Kleber, M., 1995. Atomic structure of nanocrystalline metals studied by diffraction techniques and EXAFS. Nanostructured Mater. 6, 105–114. https://doi.org/10.1016/0965-9773(95)00034-8

Wolf, D., 1989. Structure-energy correlation for grain boundaries in F.C.C. metals—I. Boundaries on the (111) and (100) planes. Acta Metall. 37, 1983–1993. https://doi.org/10.1016/0001-6160(89)90082-5

Wu, R., Freeman, A.J., Olson, G.B., 1996. Effects of carbon on Fe-grain-boundary cohesion: First-principles determination. Phys. Rev. B 53, 7504–7509. https://doi.org/10.1103/PhysRevB.53.7504

Yoshitake, M., Tsuchiyama, T., Takaki, S., 2012. Effect of Carbon and Nitrogen on Work Hardening and Deformation Microstructure in Stable Austenitic Stainless Steels. Tetsu--Hagane 98, 223–228. https://doi.org/10.2355/tetsutohagane.98.223

How to cite this article:

Ahmed Tamer AlMotasem (2018) 'An Atomistic Study on the Role of Grain Boundary Segregated Carbon and Nitrogen on the Tensile Properties of Nanocrystalline Ferrite', *International Journal of Current Advanced Research,* 07(10), pp. 16051-16057. DOI: http://dx.doi.org/10.24327/ijcar.2018.16057.2947

****